Tunnelling and Underground Space Technology 97 (2020) 103261

Contents lists available at ScienceDirect

Tunnelling and Underground Space Technology

journal homepage: www.elsevier.com/locate/tust

Temperature performance of a heat-traced utilidor for sewer and water pipes in seasonally frozen ground

Youen Pericault[a,*], Mikael Risberg[b], Maria Viklander[a], Annelie Hedström[a]

[a] Department of Civil, Environmental and Natural Resources Engineering, Luleå University of Technology, 97187 Luleå, Sweden
[b] Department of Engineering Sciences and Mathematics, Luleå University of Technology, 97187 Luleå, Sweden

ARTICLE INFO

Keywords:
Drinking water distribution
Drinking water temperature
Sewage collection
Low temperature district heating
Pipe insulation
Freeze protection

ABSTRACT

Heat-traced utility corridors (utilidors) can be used in cold regions to install the drinking water and sewer pipes in a shallow trench above the frost depth, thereby limiting excavation needs and the associated economic, social, and environmental costs. Several of these infrastructures were built in the 60s and 70s in Canada, Alaska, Russia, and Norway. More recently, a new type of heat-traced utilidor was built as a pilot project in Kiruna, Sweden to increase the viability of district heating in the area by allowing co-location of all the utility pipes in a shallow trench. Despite several reported cases of undesirably warm drinking water from full-scale projects, previous research efforts on heat-traced utilidors have mainly focused on pipe freeze protection, not on the prevention of excessive temperatures of the drinking water. To ensure comfortable drinking water in terms of taste and smell, an upper temperature limit of 15 °C is usually recommended. The objective of this study was to evaluate the long-term ability of a heat-traced utilidor to maintain sewer temperatures above 0 °C and drinking water temperatures between 0 and 15 °C. Pipe temperatures were measured continuously at two cross sections of a heat-traced utilidor located in Northern Sweden over a period of 22 months. A thermal model, set up and calibrated on the measurements, was used to simulate the impact of extraordinary cold weather conditions on the pipes' temperatures. The results showed that the utilidor could keep the pipe temperatures within the desired ranges in most cases but that special care should be taken during design to limit drinking water temperatures during the summer.

1. Introduction

In regions affected by freezing temperatures, frost can penetrate the ground down to a maximal depth usually called the frost line depending on the local climate. Seasonally frozen ground designates the soil layer situated above the frost line. Drinking water and sewer pipe networks are normally installed below the frost line to prevent any freezing of drinking water or sewage during winter. However, in regions where the frost line is deep (more than ~1.5 m), these networks are sometimes installed in seasonally frozen ground in order to limit the excavation costs (Gunderson, 1978; Hazeni et al., 1990; Mcfadden, 1990; Coutermarsh and Carbee, 1998; Bai and Wang, 2013). In this case, freeze protection measures need to be implemented and several alternatives are available to water utilities (Smith, 1996; Schubert et al., 2013; Pericault et al., 2017).

One alternative called heated utilidor is an insulated corridor where sewer, water, and possibly other utility networks are placed, and in which temperatures are kept above 0 °C with a heat-tracing system (Schubert and Crum, 1996) or thanks to heat loss from district heating lines. Heated utilidors may be of different sizes (from large enough for someone to walk in, to a compact box design). They can be installed underground or above ground and may be open or filled with insulation or sand. Several of these infrastructures were built in the 60s and 70s in Canada, Alaska, Russia, and Norway (Gunderson, 1978; Smith, 1996). More recently, a compact utilidor made of expanded polystyrene was installed in a neighbourhood of Kiruna, Sweden (Pericault et al., 2017). The latter is equipped with a heat-tracing pipe that can re-circulate part of the return water from the adjacent low temperature district heating system. A sustainability assessment of this utilidor solution in comparison to more traditional alternatives is found in Pericault et al. (2018).

While the original purpose of heated utilidors is to maintain the sewer and drinking water above 0 °C, at the same time ensuring that these systems do not excessively heat the drinking water is also

* Corresponding author.
E-mail addresses: youen.pericault@ltu.se (Y. Pericault), Mikael.risberg@ltu.se (M. Risberg), maria.viklander@ltu.se (M. Viklander), annelie.hedstrom@ltu.se (A. Hedström).

https://doi.org/10.1016/j.tust.2019.103261
Received 25 April 2019; Received in revised form 20 September 2019; Accepted 20 December 2019
Available online 08 January 2020

primordial. As recommended by the World Health Organization (2008), drinking water should be kept under 25 °C in the distribution system to limit regrowth of microorganism. However, an upper limit of 15 °C is preferable to ensure comfortable drinking water as people usually enjoy fresher water (Pangborn and Bertolero, 1972) and because temperature above 15 °C can already lead to unpleasant smells and tastes (Health Canada, 1995). The main function of heated utilidors is therefore not only freeze protection but rather to keep drinking water pipe temperature in the range 0–15 °C and sewer pipe temperature above 0 °C. In this paper, the ability of the utilidor to fulfil this technical function is referred to as temperature performance.

Scientific studies of the temperature performance of heated utilidors are scarce in the literature, even though both freezing (Smith, 1996) and over-heating problems (Leitch and Heinke, 1970, as cited in Smith,1996; Reed, 1977, as cited in Smith, 1996; Pericault et al., 2016) have been reported on these infrastructures. Kennedy et al. (1988) showed that air temperatures inside a hollow utilidor were well above 0 °C (30–40 °C) during two winters of measurements, but the resulting drinking water temperature levels were not evaluated. In Pericault et al. (2017), a heat-tracing temperature of 25 °C was found most promising to ensure good temperature performance of the utilidor of Kiruna. However, this finding derived from a short-term experiment performed under mild climatic conditions.

Hence, the objective of the present study was to evaluate the long-term temperature performance of a utilidor located in northern Sweden by (a) monitoring drinking water and sewer pipe temperatures at two cross sections of the utilidor during an extensive period and quantifying deviations from the desired temperature ranges using a degree-day approach, and (b) using a calibrated and validated thermal model of one of the cross sections to simulate temperature performances under extraordinary cold conditions.

2. Methods

2.1. Study site

The study was performed on the shallow utilidor (~1 m) of Tuolluvaara in the Municipality of Kiruna, Sweden. The climate in this area is sub-arctic and the recommended frost-free depth for water pipe installation under roads is 2.9 m. The utilidor is made of expanded polystyrene (EPS) and includes three pipe networks: drinking water, gravity sewer, and heat tracing. The purpose of the heat-tracing network is to maintain positive temperatures in the utilidor during the cold season by re-circulating warm water from the local low temperature district heating network. A more detailed description of the study site, including an aerial view, is available in Pericault et al. (2017).

2.2. Measurements

Pipes and soil temperatures were measured at two cross sections of the utilidor system from 1 November 2016 to 31 August 2018. Cross section 1 (CS1) was situated under a lawn covered by snow during winter while cross section 2 (CS2) was situated under a carport that was always free from snow. CS1 was on a pipe segment servicing two flats referred as flats 1 and 2, while CS2 was on a pipe segment servicing only flat 2. The geometries of CS1 and CS2 are presented in Fig. 1 together with the locations of temperature sensors. The soil outside the trench was silty gravelly sand at cross section 1 and crushed rocks at cross section 2. Sensors W1 and W2 were placed on the outside of the drinking water pipe while sensors S1 and S2 were placed inside the sewer pipe. Sensors H1 and H2 were placed on the outside of the heat-tracing pipe while sensors SO1 and SO2 were placed in the soil 20 cm outside the utilidor. Two soil samples were taken at each cross section in the layer of 0–45 mm crushed rocks. The soil type of these samples was found to be GW-GP (clean gravels) according to the Unified Soil Classification System. Temperatures of the drinking water pipes (W1, W2), sewer pipes (S1, S2), and heat-tracing pipes (H1, H2) were recorded every four minutes, while the soil temperatures (SO1, SO2) were measured every hour. Digital temperature sensors GI-695 supplied by Intab were used. The measurement accuracy provided by the manufacturer is ± 0.5 °C, in the range −10 °C + 80 °C. Measurements were logged with the Intab WiSensys system and continuously uploaded for storage on the Intab cloud. Hourly outside air temperatures were retrieved from the Swedish Meteorological and Hydrological Institute (SMHI) open-data platform (SMHI, 2018) for the period 1/11/16 to 31/08/18.

2.3. Operation of the heat-tracing system

A lower soil temperature (sensors SO2) threshold of 2 °C was used as activation criteria for the heat-tracing system. During the first winter (18/10/16–16/05/17), the pump re-circulating return water from the low temperature district heating network into the heat-tracing network was continuously in operation. Because the district heating return water temperature was most often above the desired range of 25–30 °C, a chiller placed just downstream the heat-tracing pump was used to cool down the water to this temperature range. During the second winter, an improved strategy for regulating the heat-tracing system was used to increase resource efficiency of the system. A timer was installed on 16/10/17 to operate the heat-tracing pump intermittently, and the chiller was not activated. Further improvements to the heat-tracing system were carried out from 05/11/17 to 10/12/17, including installation of anti-return valves into the network, and the system was in full operation from 11/12/17 until 25/04/18.

2.4. Modelling

2.4.1. Initial model

A two dimensional (2D) finite volume model of cross section 2 (Fig. 1) was set up using the thermal modelling software ANSYS CFX. The reason for selecting cross section 2 was the absence of an insulating layer above the utilidor (no snow or turf), making the section more vulnerable to cold and hot weather events than cross section 1 (snow during winter, and turf). The geometry and soil layers presented in Fig. 1 were used. Boundary conditions on the right and left of the model were set as adiabatic, while a geothermal heat flux of 0.08 W/m^2 (Bishop et al., 2014) was set at the bottom of the model. The total width and height of the numerical model were 11.7 m and 6 m. The average element size of the discretization mesh was 8 mm inside the water-sewer utilidor and 30 mm in the rest of the cross section.

The thermal parameters of the layer of 0–45 mm crushed rocks (identified as GW-GP soil type according to the USCS classification) were considered temperature dependent as this material can hold water and therefore has different thermal properties when frozen, unfrozen and during freezing/thawing due to latent heat. The frozen and unfrozen thermal conductivities were determined with Johansen's method (Johansen, 1975) considering a porosity of 0.265 (ASRTE, 1999), a particle density of 2660 kg/m^3, a volumetric water content of 0.06 (assumed equal to field capacity of coarse sand), and a quartz content of soil particles of 0.45 (Johansen, 1975). The frozen and unfrozen heat capacities of the layer of crushed rock were determined with the method described in Andersland and Ladanyi (1994). The unfrozen water content curve proposed by Geo-slope (2010) for gravels was then used to derive temperature dependent curves for the thermal properties of the crushed rock layer (Fig. 2), considering a value of 333.7 kJ/kg for the latent heat of fusion/solidification of water. These curves were used as input parameters in the initial finite volume model.

For the other material composing cross section 2, the same thermal conductivity (concrete: 1.7 W/m K; EPS: 0.035 W/m K; polyethylene pipes: 0.54 W/m K) and heat capacity values (concrete: 1.2 MJ/m^3 K; EPS: 0.032 MJ/m^3 K; polyethylene pipes: 1.8 MJ/m^3 K) as in Pericault et al. (2017) were used. The gravity sewer pipe was considered empty

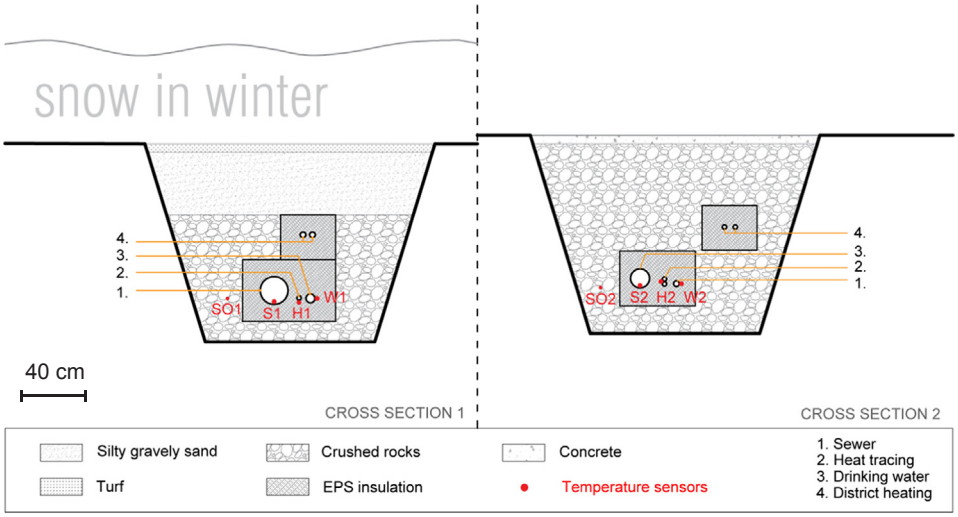

Fig. 1. Geometry of the studied cross sections and position of the temperature sensors.

(without wastewater flow) and a Nusselt number of 7 was used for the in-sewer air to account for natural convection (Martini and Churchill, 1960). This corresponded to a value of 0.168 W/m K for the effective thermal conductivity of in-sewer air. The drinking water pipe was modelled as filled with standing-still water (no flow). This scenario with no water consumed and no sewage discharged was considered because it corresponds to the worst flow scenario concerning freezing and overheating risks. A simulation was run with the initial model for the period 1/11/2016–31/7/2017 with a time step of 1 day. The temperature at the upper boundary of the model (soil surface) was set equal to the measured outdoor air temperature. This simplified approach was selected because it yielded soil temperatures very similar (mean absolute error of 0.10 °C at sensor location SO2 during the calibration period) to the ones we obtained with a more complete approach (Gwadera et al., 2017) that accounted for the effect of wind on the heat transfer at the soil surface. The measured heat-tracing pipe temperature (Fig. 1, sensor H2) was applied on the outer surface of the heat-tracing pipes in the model. The measured district heating pipe temperatures were also applied on the outer surface of these pipes in the model. The outputs of the model were time series for the drinking water, sewer and soil temperatures for the same locations as sensors W2, S2 and SO2.

To estimate if the model size was large enough to avoid boundary effects, a simulation was run with twice the width and height of the initial model. The results showed an average difference of 0.11 °C for the cold water temperature at each time step compared with the size used in the initial model. The discretization error was estimated by running the initial model with 3.75 times more elements, and the temperature difference for the cold water temperature was on average 0.06 °C between the refined and original mesh at each time step.

2.4.2. Calibration

The calibration was performed in four stages with temperature data from the period 1/11/2016 to 31/7/2017. For each stage, the coefficient of determination R^2 as given by Nash and Sutcliffe (1970) and the root mean square error (RMSE) were used as indicators of model performance. Firstly, three physical parameters of the soil layer of crushed rocks were calibrated using the measurements from sensor SO2 (Fig. 1). These parameters were the quartz content of soil particles (q), the soil porosity (n), and the volumetric soil water content (W). For the quartz content, values of 0.45 (initial value), 0.23 (50% decrease), and 0.68 (50% increase) were considered. For soil porosity, values of 0.265 (initial value), 0.195 (30% decrease), and 0.335 (30% increase) were considered. For the volumetric water content, values of 0.06 (initial value), 0.03 (50% decrease), and 0.09 (50% increase) were considered. Parameter values giving the best model performances were selected and kept for the remainder of the calibration process. In the second stage, the thermal conductivity of the EPS material (λ_{EPS}) was calibrated using the measurements from sensor W2 (right of drinking water pipe, Fig. 1). The following λ_{EPS} values were considered: 0.035 W/m K (initial value), 0.046 W/m K (30% increase), and 0.053 W/m K (50% increase). The λ_{EPS} value giving the best model performance was selected and kept for the next stages of the calibration process. In a third stage, the effective thermal conductivity of in-sewer air (λ_{air}) was calibrated using the measurements from sensor S2 (inside the sewer pipe, Fig. 1). The following λ_{air} values were considered: 0.168 W/m K (initial value), 0.084 W/m K (50% decrease), and 0.252 W/m K (50% increase). The

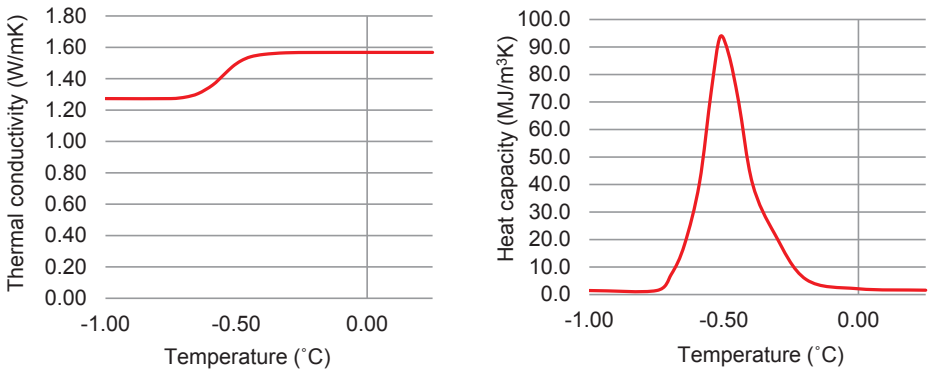

Fig. 2. Thermal conductivity (left) and heat capacity (right) of the crushed rock layer (0–45 mm) as a function of temperature. The curves remain constant above 0 °C and below −1 °C.

λ_{air} value giving the highest model performances was selected and kept for the final stage of the calibration process. In this stage, the location of sensor S2 inside the sewer (θ) in the model was also adjusted to maximize model performances with regards to sewer temperature prediction. θ corresponds to the angle between the pipe bottom and the sensor location on the inner pipe wall, as this sensor was laid but not attached inside the sewer pipe and could lean slightly on the right or left part of the pipe wall.

2.4.3. Validation

The validation period (1/8/2017–31/7/2018) was divided in two: sub-period 1 (1/8/2017–31/1/2018) where no water/wastewater flow was expected (no tenants in serviced flat 2) and sub-period 2 (1/2/2018–31/7/2018) where water/wastewater flows were expected (tenants living in serviced flat 2). This was because model performances were expected to differ significantly between the sub-periods, as it was set up and calibrated for the no-flow case (corresponding to sub-period 1). The calibrated model was run for the whole validation period (1/8/2017–31/7/2018), and the coefficient of determination R^2 was computed at sensor location S2, W2, and SO2 for each sub-period.

2.4.4. Simulation of extraordinary cold scenario

The temperature record for Kiruna Airport weather station (1957–2016) was examined in order to find the 31-day and 7-day periods with the lowest average temperature, referred to as extraordinary cold scenario in this paper. The coldest 31-day period recorded was 13/12/1986 to 12/1/1987 with an average air temperature of −25.3 °C. The coldest 7-day period was included in the coldest 31-day period and had an average air temperature of –33.8 °C. The calibrated model was then run for the winter 1986–1987 from 15 October to 15 April (typical period when the heat-tracing system is required). The temperature of the outer surface of the heat-tracing pipe was set constant and equal to 20, 25 and 30 °C (3 model runs). The geometry of the cross section was modified by removing the upper heat-tracing pipe. This was because the stacked heat-tracing pipes is a particularity of cross section 2, while most of the utilidor sections are equipped with only one heat-tracing pipe (Pericault et al., 2017).

2.5. Evaluation of temperature performance

For the measured time series of drinking water and sewer pipe temperatures (sensors W1, S1, W2, S2), hourly averages were calculated from the raw data (time step of 4 min). In cases of gaps in the data, the hourly average was calculated with the available data point inside the considered hour, given that at least one data point was available. For the modelled time series at sensor locations W1, S1, W2, and S2, only daily temperatures were available. Hourly time series were constructed by attributing the daily average temperature to all the hours inside the considered day. For both measured and modelled time series of hourly pipe temperatures, a calculation method based on degree-days was used to evaluate indicators of temperature performances on a monthly basis. An indicator of freezing risk D_0 (°C day) was computed for both the sewer and drinking water pipe and corresponded to the amount of degree-days below 0 °C. An indicator of discomfort for the drinking water consumer, D_{15} (°C day) was computed for the drinking water pipe only and corresponded to the amount of degree-days above 15 °C.

3. Results

3.1. Measurements

The drinking water and sewer pipe temperatures measured from November 2016 to August 2018 are shown in Fig. 3a (cross section 1) and 3b (cross section 2). The heat-tracing temperature and status of the heat-tracing system (on or off) are shown in Fig. 3c, while the measured outdoor air and soil temperatures are shown in Fig. 3d. The deviation of drinking water/sewer pipes temperature from the 0–15 °C/ > 0°C temperature ranges were quantified for both cross sections using indicators D_0 and D_{15} (Table 1).

Temperatures of the drinking water pipes were not measured below 0 °C during the experimental period (November 2016-August 2018) as seen in Fig. 3 and Table 1. When the heat-tracing system was activated (winter time), drinking water pipe temperatures were most frequently in the range 10–15 °C when the serviced flats were unoccupied and in the range 5–10 °C when tenants were living in these flats. When the heat-tracing system was not activated, the drinking water pipe temperatures varied mainly in the range 5–15 °C following the outdoor air temperature variations.

The drinking water pipe temperature exceeded the comfort limit (15 °C) several times during the experimental period, as shown by indicator D_{15} (Table 1). Some of these deviations were smaller than or equal to 1°-day and cannot be seen in Fig. 3. A larger deviation occurred in October and November 2017 with, in total, 22.8 and 68 degree-days above 15 °C at cross sections 1 and 2. This event can also be seen clearly in Fig. 3, with drinking water pipe temperatures even exceeding 20 °C at cross section 2. The reason for this over-heating event was counter-flows in the heat-tracing pipe network that occurred during improvement works on the heat-tracing regulation system as described in part 2.3.

Another deviation occurred during the summer of 2018 at cross section 1 with 39 degree-days above 15 °C (Table 1). The average daily temperature of the drinking water pipe reached 18.9 °C on 5/8/2018, as visible in Fig. 3a. The soil temperature was in the range 10–15 °C during the summer of 2018 at cross section 1. The drinking water pipe temperatures at cross section 2 also exceeded 15 °C during the summer 2018 but only for a few hours (0.8 degree-days for the whole month of August). This did not lead to daily averages above 15 °C as seen in Fig. 3b. The soil temperature was in the range 10–17 °C during the summer at cross section 2. For the sewer pipe, the measured temperatures were most often below 10 °C, except during summer time and at cross section 1, when tenants were present in the serviced flats (Fig. 3a). The soil temperatures were warmer during winter time at cross section 1 (0.5–2 °C) than at cross section 2 (−10 to 0 °C) due to the insulation provided by the snow cover at cross section 1. Overall, the drinking water was colder and sewer warmer when tenants were living in the serviced flats than when they were not (Fig. 3). As seen in Fig. 3b, the sewer pipe temperature at cross section 2 dropped below 0 °C several times during January and February 2017. As shown in Table 1 by indicator D_0, it corresponded to a deviation of 14 degree-days from the lower temperature limit of 0 °C. However, this was due to cold outside air infiltration from a manhole along the cable of the sewer temperature sensor. This problem was fixed in February 2017 by making the cable passage to the sewer pipe air-tight.

3.2. Model calibration and validation

A summary of the calibration process is presented in Table 2. The indicators of model performance (R^2 and RMSE) with regards to soil, water pipe, and sewer pipe temperature prediction are shown in Table 2 for the different tested parameter changes. The initial model predicted the soil temperatures well (R^2 = 0.96; RMSE = 1.06 °C). During the first calibration stage, changes in quartz content of soil particles (q) and soil porosity (n) did not improve the performance indicator values. Initial q and N values were therefore kept. Increasing the volumetric soil water content W from 0.06 to 0.09 (+50%) improved marginally the R^2 and RMSE value of soil temperature predictions but this increase was only visible on the third decimal (values are rounded to two decimals in Table 2). The W value of 0.09 was selected as the calibrated value. Stage 2 resulted in a calibrated value of 0.046 W/m K (30% increase) for the thermal conductivity (λ_{EPS}) of EPS insulation. This increased the R^2 value for the drinking water pipe temperature from 0.54

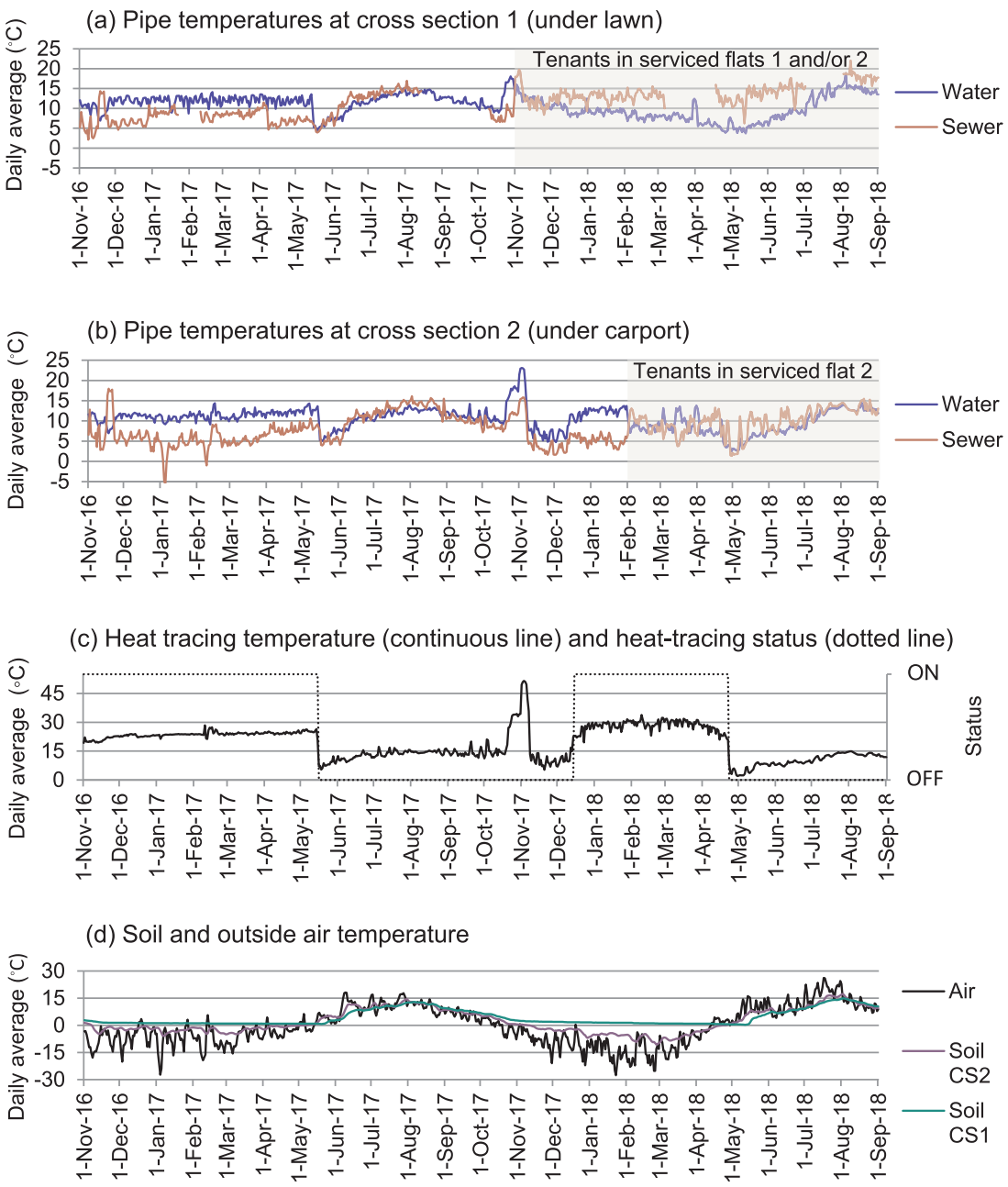

Fig. 3. Measured temperatures from November 2016 to August 2018: water and sewer pipes at two cross sections of the utilidor (a, b), heat-tracing (c), outside air and soil (d). The status of the heat-tracing system (on/off) is also represented in (c). In (a) and (b), the presence of tenants inside the serviced flats is indicated by the grey areas.

to 0.60. In the third calibration stage, the effective thermal conductivity (λ_{air}) of in-sewer air was increased by 50% (new value 0.252 W/m K), which improved the R^2 value for the sewer pipe temperature from 0.42 to 0.46. Finally, in the fourth stage, the temperature sensor position (Θ) was increased from 0° to 60°, which improved the R^2 value from 0.46 to 0.60 for the sewer pipe temperature.

The modelled and measured temperature time series of the drinking water pipe, sewer pipe, and soil are presented in Fig. 4 for the calibration and validation periods. The difference in soil temperature between the initial model and the model with calibrated soil parameters is not appreciable in Fig. 4a (lines are overlapped). In general, the model with calibrated soil parameters predicted the soil temperature well during the calibration and validation periods, with high R^2 values of 0.96 and 0.97 (Fig. 4). However, this model underestimated the soil temperature by more than 3 °C during 5 days in January and February 2018. The largest modelling error was of 3.5 °C during the calibration period (15/11/16) and −4 °C during the validation period (23/1/18).

For the temperature of the drinking water pipe, the improvement in R^2 value (from 0.54 to 0.60) offered by adjusting the thermal conductivity of EPS insulation is not visible on the temperature time series (lines overlapped in Fig. 4b for the "soil calibrated" and "fully calibrated" models). During the calibration period, the fully calibrated model showed deviation smaller than 2 °C for 95% of the drinking water pipe temperature measurements. During the validation subperiod 1 (without tenants in flat 2), the model had a relatively high R^2 value of 0.69 for the drinking water pipe temperature. This value was higher than for the calibration period (0.60). This can be attributed to the very good performances of the soil temperature model for the period September to November 2017 (Fig. 4a). When limited to the period December 2017 to January 2018, the coefficient R^2 was

Table 1
Temperature deviations from target temperature ranges (degree-days) for pipes at cross section 1 (under lawn) and 2 (under carport). Only the months where at least one indicator was positive are shown. Parentheses indicate that the deviation occurred during improvement or maintenance work on the technical system. Hyphens indicate lack of data.

		D_0: sewer pipe below 0 °C [°C day]		D_0: water pipe below 0 °C [°C day]		D_{15}: water pipe above 15 °C [°C day]	
		CS 1	CS 2	CS 1	CS 2	CS 1	CS 2
2017	January	–	(12)	0	0	0	0
	February	–	(2.0)	0	0	0.75	0.042
	July	0	0	0	0	0.13	0
	August	–	0	0	0	0.33	0.13
	September	–	0	0	0	0	0.042
	October	–	0	0	0	(17)	(24)
	November	0	0	0	0	(5.8)	(44)
	December	0	0	0	0	0.17	0.29
2018	January	0	0	0	0	0	0.13
	July	–	0	0	0	13	0
	August	0	0	0	0	26	0.80

considerably lower (0.23). During validation sub-period 2, the performances of the calibrated model were lower than in validation sub-period 1 with a R^2 value of 0.51. This could be explained by the consumption of drinking water by the tenants, which was not taken into account in the model (each water consumption brings colder water from the deeper upstream pipes). This is visible in Fig. 4b, with deviations of up to 5 °C during April 2018.

For the sewer pipe temperatures, the impact of the calibration was more noticeable on the temperature time series. The model with only soil parameters calibrated (dashed line in Fig. 4c) was most often colder than the observations during the calibration period. However, the fully calibrated model (continuous line in Fig. 4c) was often confounded with the measured temperature time series during the calibration period, except during three events where warm water was discharged in the sewer (November 2016) or when cold air infiltrated along the cable of the temperature sensor (January and February 2017). The fully calibrated model also performed well regarding sewer pipe temperatures during the validation sub-period 1 (R^2 value of 0.83, better than for calibration). This can also be explained by the very good performances of the soil temperature model for the period September to November 2017. The R^2 coefficient was lower (0.05) for the period December 2017 to January 2018. As expected, the model performance was very low during the validation sub-period 2, with a R^2 value of −0.62 and deviations often larger than 5 °C. This could be explained by the discharge of warm water in the sewer by the tenants of flat 2 during this period, which was not accounted for in the model.

3.3. Modelled pipe temperatures under exceptionally cold winter conditions

The use of the calibrated model for the period 15/10/1986 to 15/4/1987 (including the coldest week and month ever recorded in Kiruna) indicated that drinking water pipe temperatures would have remained above 0 °C during that period (> 1 °C, see Fig. 5). The results applied for cross section 2 (no snow cover) with one heat-tracing pipe constantly at 20, 25 or 30 °C as well as no drinking water consumption nor sewage discharge. The simulation indicated also that, for a heat tracing level of 25 °C, the sewer pipe temperature would have dropped below 0 °C during 14 days (Fig. 5) corresponding to a deviation of 47 degree-days. For a higher heat tracing level of 30 °C, this deviation was still observed and represented 24 degree-days. For a lower heat tracing level of 20 °C, sewer pipe temperatures below 0 °C were observed more frequently, representing a deviation of 111 degree-days. This does not directly mean that freezing would occur in cases of sewage flow, as sewage is discharged well above 0 °C and has a higher heat capacity than the surrounding cold PVC pipe and EPS insulation. However, it could cause clogging due to freezing if solids were transported intermittently in the sewer lateral due to poor self-cleansing properties. The simulation indicated that the soil temperature would have been −21 °C at the coldest, after 7 days with air temperatures below −30 °C.

4. Discussion

4.1. Temperature performance

The temperature measurements and the simulation indicated that the studied utilidor system was correctly designed to prevent freezing of the drinking water under the studied conditions. Indeed, drinking water pipe temperatures of less than 0 °C were not measured during the

Table 2
Summary of the calibration process for the period 1/11/16–31/7/18. Final calibrated parameters are depicted in bold. The arrow represents the workflow of the 4-stage calibration process.

Stage	Parameter change	New value	Soil		Water pipe		Sewer pipe	
			R^2	RMSE	R^2	RMSE	R^2	RMSE
0	None (initial set: q=**0.45**; n=**0.265**; W=0.06; λ_{EPS}=0.035W/mK; λ_{air}=0.168W/mK; Θ=0°)	-	0.96	1.06				
1	q -50%	0.23	0.96	1.14				
	q +50%	0.68	0.96	1.11				
	n -30%	0.20	0.95	1.17				
	n +30%	0.34	0.94	1.34				
	W -50%	0.03	0.95	1.20				
	W +50%	**0.09**	0.96	1.06	0.54	1.16		
2	λ_{EPS} +30%	**0.046** W/m.K			0.60	1.09	0.42	2.75
	λ_{EPS} +50%	0.053 W/m.K			0.55	1.16		
3	λ_{air} -50%	0.084 W/m.K					0.42	2.73
	λ_{air} +50%	**0.252** W/m.K					0.46	2.64
4	Θ +30°	30°					0.57	2.36
	Θ +60°	**60°**	0.96	1.06	0.60	1.09	0.60	2.28
	Θ +90°	90°					0.60	2.28

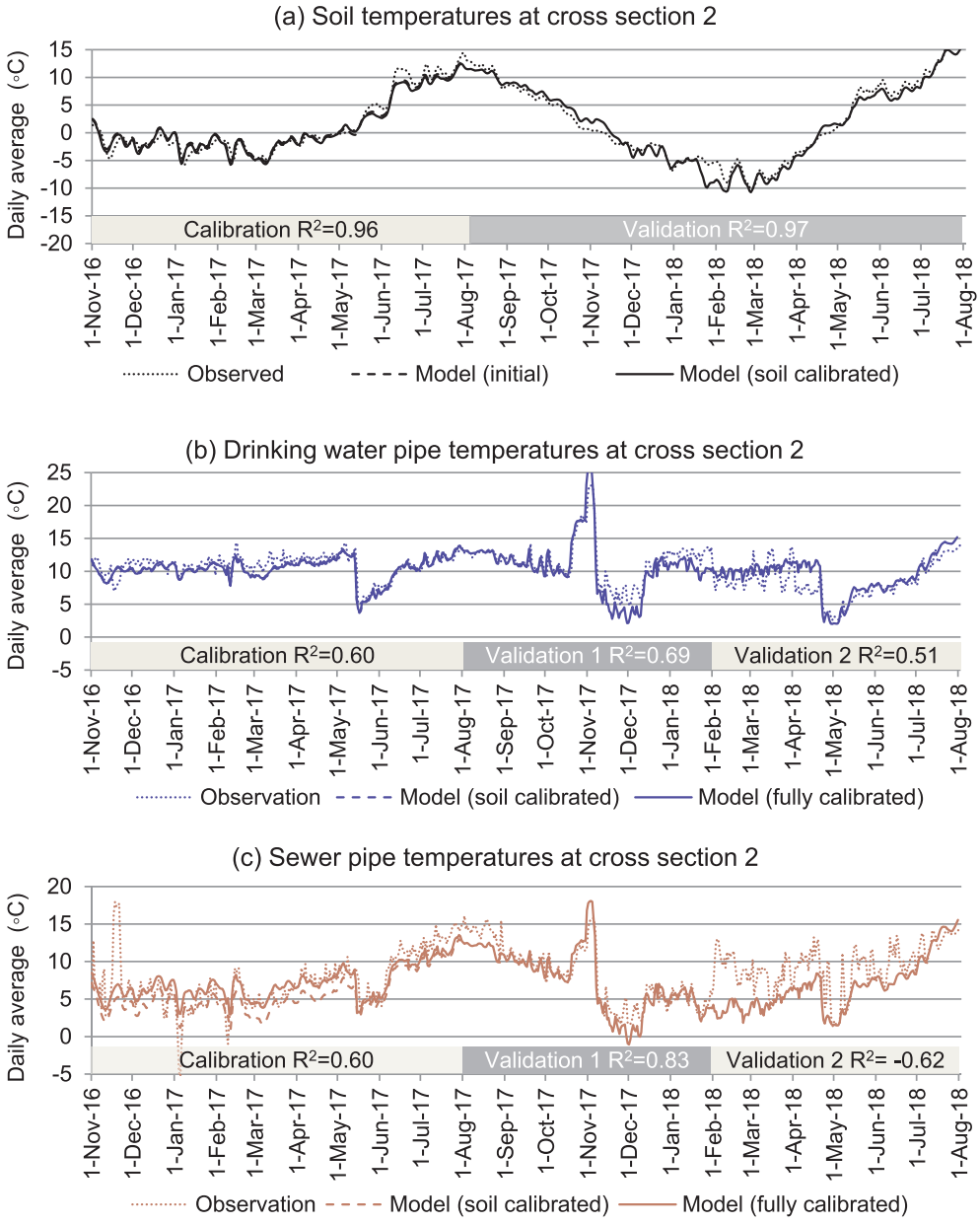

Fig. 4. Modelled and observed temperatures at cross section 2 for the soil (a), drinking water pipe (b), and sewer pipe (c). R^2 values are given for the soil calibrated model in (a) and fully calibrated model in (b and c).

experimental period and the model that proved reliable for drinking water temperature prediction (R^2 value of 0.69 during validation period) indicated that the drinking water pipe temperature would have remained above 3.5 °C during the extraordinary cold weather conditions simulated. Moreover, the model corresponded to the worst-case scenario for freeze protection with regards to snow cover (no snow cover), and sewage flow (no flow). The prevention of drinking water freezing is, however, conditioned by the heat-tracing temperature, which should be above 20 °C even at cross sections furthest from the district heating house station. This needs to be considered in the regulation setting of the heat-tracing system, especially since temperature drops in heat-tracing pipes are larger during very cold periods due to colder soil temperatures. The calibrated model indicated that the sewer pipe would be at negative temperatures during extraordinary cold weather conditions if no sewage were discharged and the heat-tracing pipe temperature was within the interval 20–30 °C. This would not necessarily lead to freezing in case of a discharge, as the warm sewage has to cool down to 0 °C before ice starts to build up on the pipe wall. This may only occur over long distances since the EPS material limits the heat loss to the surrounding soil. However, to discard any freezing risk, it would be preferable, during very cold events, to operate the heat-tracing system at temperatures near the upper bound of the 20–30 °C interval. This appears possible as return temperatures of 30 °C are normally available in low temperature district heating systems (Lund et al., 2014).

The results suggest that the studied utilidor system is able to keep drinking water under 15 °C during most of the year. During summers, deviations can occur because the shallow installation means that soil temperatures can reach 15 °C at the level of the pipes (in this study 17.3 °C at cross section 2 in August 2018). This was observed during a cohesive period of 27 days during the summer 2018 when drinking water pipe temperatures were in the range 15–19 °C at cross section 1 and 13–15 °C at cross section 2. The drinking water temperature at cross section 1 was then often above the 15 °C recommendation to prevent bad taste and odour (Health Canada, 1995) but not above 25 °C (limit for health risks, World Health Organization, 2008). However, this

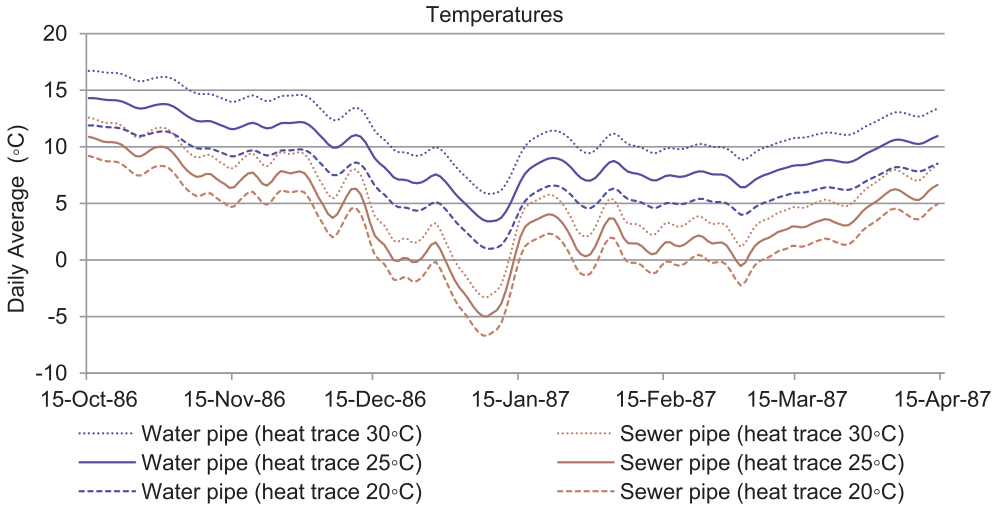

Fig. 5. Simulated drinking water and sewer pipe temperatures for the period 15/10/1986–15/04/1987 for different heat tracing temperatures.

deviation could not be explained purely by too high soil temperature as the latter reached only 14.9 °C at cross section 1 during the summer 2018. A plausible reason is that the district heating utilidor was situated directly on the top of the water-sewer utilidor at cross section 1 (Fig. 1). Possible measures to limit drinking water temperature during summer would be to install the utilidor deeper, to avoid direct contact between the water-sewer and the district heating utilidors, or to increase the insulation thickness to limit the warming process of the cold drinking water by the surrounding soil in summer. This would be particularly relevant for lateral connections where residence time of the water is higher than in the rest of the network.

4.2. Representativity

The summer of 2018 in Kiruna was exceptionally warm, with two periods of 4 and 5 respectively consecutive days measured above 20 °C. The normal value for the longest period of consecutive days above 20 °C in Kiruna for the period 1991–2013 is 1 day (Berglöv et al., 2015). However, this normal value is expected to increase to 2–4 days by 2050 and 6 to 12 days by 2100, depending on the severity of climate change (Berglöv et al., 2015). This means that the problem of too warm drinking water observed during the summer 2018 needs to be addressed in the future design of these types of systems, as the conditions observed during the summer 2018 are likely to occur regularly and increasingly during their lifetimes. This holds for cold climate regions with warmer summer than in Kiruna. In more temperate areas, the problem of too warm drinking water during summer has been observed for conventional drinking water networks installed at the frost depth (Blokker and Pieterse-Quirijns, 2013; Agudelo-Vera et al., 2014).

The winter 2017–2018 in Kiruna was about 1 °C colder than the norm for the period 1991–2013, while the winter 2016–2017 was very mild with an average air temperature 5 °C above the normal (Berglöv et al., 2015). However, an increase of the normal winter air temperature by 5 °C or more is forecasted by 2070 due to climate change (Berglöv et al., 2015). Consequently, the pipe temperatures observed during the winter 2016–2017 seem to be more representative of the system's normal behaviour in the long term. However, these temperatures (shown in Fig. 3) were measured in no-flow conditions for the drinking water and sewer pipe. Regular water consumption and sewage discharge patterns have shown to be beneficial to temperature performances in this study (i.e. colder drinking water, warmer sewage) as seen in Fig. 3. The forecast of a 5 °C increase in winter air temperatures in Kiruna also suggests that the likelihood of occurrence of extraordinary winter conditions, as cold as in 1986–1987, will decrease.

The studied cross sections were both situated in the downstream part of the heat-tracing system. A large part of the system was therefore exposed to slightly higher heat-tracing temperatures that at cross sections 1 and 2. However, drinking water pipe temperatures did not increase during drinking water consumption, which suggests that temperature performance was not worse in the more upstream cross sections. Greater temperature drops along the heat-tracing pipe can be expected in larger systems and should be addressed during design to ensure that freeze protection in the most downstream cross section is possible without overheating the upstream ones. In term of geometry, cross section 1 represented the case of a pervious surface covered by snow during winter (e.g. garden lawn, public grass strips), and cross section 2 represented an impervious surface that is snow-free year round (e.g. road, pavement, parking).

4.3. Thermal modelling of underground box-utilidors

Soil thermal parameters of the utility trench can vary with time and location and usually require more effort to evaluate than the material found in the utilidor. The investigated EPS insulation and the plastic pipes were manufactured in a controlled environment, while filling aggregates can be produced from various rock types, are compacted on site, and can vary considerably in moisture content. If the natural soil is also used for filling the trench, thermal properties of the utility trench can vary even more from one location to another. In this study, knowledge of the soil type obtained from field samples appeared sufficient to set up a reliable soil temperature model ($R^2 = 0.96$, RMSE = 1.06 °C) by direct estimation of the quartz content (q), porosity (n), and water content (W) values from the literature. The access to soil temperature measurements (sensor SO2) to calibrate the model allowed validation of the choice of initial quartz content (q) and porosity (n) values, but did not significantly improve model performances ($R^2 = 0.96$, RMSE = 1.06 °C). Only the volumetric water content W was increased from 6% to 9% during the calibration process and the impact on the RMSE value was 0.002 °C, which is negligible in relation to the sensor accuracy of ± 0.5 °C. These values (W = 6% and 9%) corresponded to gravimetric water content by dry weight of 3% and 5%. The latter two are slightly lower than previous findings by Kuznetsova (2015) where water contents between 5.9 and 10.4% were found for crushed rocks with fine (< 0.063 mm) contents below 6% sampled from road foundations in Norway. The share of fine material (< 0.071 mm) in the samples taken in the crushed rock layer above the utilidor were below 7%. The model performances were not sensitive to changes in volumetric soil water content (Table 2) but only values between 3 and 9% were considered because the studied cross section was under a car port (i.e. sheltered from rain and snow). The volumetric

water content was therefore expected to be relatively constant and close to the field capacity of the crushed rock layer. Similar results can be expected under impervious surfaces in flat areas (e.g. road asphalt) but not under pervious surfaces such as turf, where the water content varies with precipitation and can reach higher values close to the porosity of the soil layer. The performance of the soil temperature model was affected more by changes in quartz content of the soil particles than changes in soil porosity. However, variations of ± 50% were considered for the quartz content (almost matching the 0.2–0.6 range proposed by Johansen (1975) while variations of ± 30% were considered for soil porosity (almost matching the range of 0.21–0.32 proposed in ASRTE (1999) for GW-GP soil type). If the soil type is not known and a broader range of porosity values is to be considered, the estimation of soil porosity may be as or more important for model performances than the estimation of the quartz content. Porosity depends on the grain size distribution and level of compaction of crushed rock layer, while the quartz content depends on the mineral composition of the rock mass that was crushed (Johansen, 1975). The calibrated value of 45% (same as initial) for the quartz content of the soil particles is relatively high considering that the GW-GP soil type in this study is not natural gravel but crushed rocks. According to Sundberg (1991), the quartz content of granite, the most common rock type in Sweden, should be between 20 and 40%. However, a quartz content value of 23% was used during the calibration process and did not improve model performance.

The thermal conductivity of the EPS insulation (material of the utilidor) is dependent on temperature (Gnip et al., 2012) and moisture (Lakatos, 2013). In this study, a value of 0.046 W/m K was found after calibration on the drinking water pipe temperature measurements (an increase of 30% of the initial value of 0.034 W/m K). This value is compatible with the findings of Cai et al. (2018), where field specimens of EPS with a density ≥ 30 kg/m^3 (density of the EPS on the pilot site is 30 kg/m^3) could suffer a thermal conductivity increase of 30% if the volumetric moisture content had reached approximately 6%. In the same study, the moisture content of EPS specimens of that density were between 1 and 12.5% after 1 to 13 years in the field in underground applications (EPS in the present study had been 3 years in the ground at the time of the experiment). However, since the calibration of this parameter was performed on the drinking water pipe temperature measurements, the EPS thermal conductivity value giving the best fit could be compensating for other factors. This could include heat loss at the interaction between the EPS utilidor and the surrounding soil, deviations of the soil temperature model, and/or errors in the thermal conductivity of the PE drinking water pipe. For the thermal conductivity of in-sewer air, an increase of 50% of the initial value gave the best fit to the sewer temperature measurements. This corresponds to a Nusselt number of 10.5, which according to Martini and Churchill (1960) is found locally inside the pipe for temperature differences between 2 and 200 °C. This Nusselt number value may correspond to the local condition where temperature sensor S2 was installed. However, the average value of 7 for the Nusselt number over the entire pipe section (Martini and Churchill, 1960) would be more relevant to model the impact of the sewer pipe on the overall heat transfer from the heat-tracing pipe to the surrounding soil.

The use of a model without drinking water or sewage flow appears relevant to assessing the functionality of the system during worst-case conditions, which is valuable for design purposes. Including these flows in the model would be preferable if the focus is to assess pipe temperature during the regular functioning of the system (as in validation sub-period 2).

5. Conclusion

In this paper, the temperature performance of two cross sections of a heat-traced utilidor installed in seasonally frozen ground was evaluated using temperature measurements, and a thermal model calibrated on these measurements. Temperature performance corresponded to the ability of the system to keep drinking water temperatures in the range 0–15 °C and sewer temperature above 0 °C. During the experimental period of 22 months, these temperatures were inside the desired ranges at both cross sections, except for 24 days during the summer 2018 when the drinking water temperatures were above 15 °C at cross section 1. Three other deviations (drinking water above 15 °C in October–November 2016, and sewer below 0 °C in January/February 2017) were observed, but occurred during maintenance or improvement works on the technical system.

The calibrated model showed that the drinking water temperature would have stayed above 0 °C during the coldest month and coldest week ever recorded at the study site location. The simulations also showed that, under these extreme conditions, the sewer pipe would have been under 0 °C for 14 days in cases of no sewage flow in the pipe (e.g. lateral connection of a villa whose tenants are on holiday) and for a heat tracing temperature of 25 °C (regular case). Regulating the heat-tracing temperature to 30 °C or more in cases of very cold ground would be an option to mitigate risks of clogging-due-to-freezing in the sewer pipe.

In light of the predictions of warmer summers in cold climate regions due to climate change, special emphasis should be put on the design of shallow heat-traced utilidors to limit the drinking water temperatures during summer. While freezing problems during winter can sometimes be addressed by adapting the regulation of the heat-tracing system, this is not the case for problems of too warm drinking water in the summer.

The satisfactory temperature performances observed during most of the heat-tracing period were conditioned by the temperatures of the heat-tracing pipe, which were in the range 20–32 °C. Ensuring adequate temperature level at all sections of a utilidor, despite the temperature drop along the heat-tracing pipe, should be addressed during design, especially for larger systems than the one studied in this paper (more than nine houses).

Finally, 2D thermal modelling using a finite volumes solver, together with Johansen's method to estimate soil thermal parameters, proved to be a relevant approach to predict pipe temperatures based on outdoor air and heat-tracing temperatures for a trench under an impervious surface. It appeared possible to set up a reliable soil temperature model without calibration data if estimations of soil textures inside and around the trench are available.

Declaration of Competing Interest

The authors declare that they have no known competing financial interests or personal relationships that could have appeared to influence the work reported in this paper.

Acknowledgements

The present study was conducted with financial support of Sweden's Innovation Agency (Vinnova) through the Attract project (No. 2014-04287), and the Swedish Research Council (Formas) through the Alice project (No. 2011-1710).

Appendix A. Supplementary material

Supplementary data to this article can be found online at https://doi.org/10.1016/j.tust.2019.103261.

References

Agudelo-Vera, C., Blokker, M., Pieterse-Quirijns, I., 2014. Early warning systems to predict temperature in the drinking water distribution network. Procedia Eng. 70, 23–30. https://doi.org/10.1016/j.proeng.2014.02.004.

Andersland, O.B., Ladanyi, B., 1994. An Introduction to Frozen Ground Engineering.

Chapman & Hall, New York.
ASRTE, 1999. Swiss Standard SN 670 010b, Characteristic Coefficients of soils. Association of Swiss Road and Traffic Engineers.
Bai, L., Wang, Y., 2013. Numerical calculation of insulating layer thickness of rural water supply pipe in permafrost regions. Adv. Mater. Res. 864–867, 2022–2026.
Berglöv, G., Asp, M., Clausen, S.B.-, Björck, E., Mårtensson, A.J., Nylén, L., Ohlsson, A., Persson, H., Sjökvist, E., 2015. Future climate in Norrbotten county (Framtidsklimat i Norrbottens län, in Swedish). Klimatologi 16.
Bishop, M.P., Bush, A.B.G., Furfaro, R., Gillespie, A.R., Hall, D.K., Haritashya, U.K., Shroder, J.F., 2014. Theoretical Foundations of Remote Sensing for Glacier Assessment and Mapping, in: Kargel, J.S., Leonard, G.J., Bishop, M.P., Kääb, A., Raup, B.H. (Eds.), Global Land Ice Measurements from Space. Springer Berlin Heidelberg, Berlin, Heidelberg, pp. 23–52. https://doi.org/10.1007/978-3-540-79818-7_2.
Blokker, E.J.M., Pieterse-Quirijns, E.J., 2013. Modeling temperature in the drinking water distribution system. J. Am. Water Work. Assoc. 105, E19–E28. https://doi.org/10.5942/jawwa.2013.105.0011.
Cai, S., Zhang, B., Cremaschi, L., 2018. Moisture behavior of polystyrene insulation in below-gradeapplication. Energy Build. 159, 24–38.
Coutermarsh, B., Carbee, D., 1998. Frost-shielding methodology and demonstration for shallow burial of water and sewer utility lines. Cold Reg. Res. Eng. Lab. Rep. 98–104.
Geo-slope, 2010. Thermal Modeling with TEMP/W 2007.
Gnip, I., Vėjelis, S., Vaitkus, S., 2012. Thermal conductivity of expanded polystyrene (EPS) at 10 °C and its conversion to temperatures within interval from 0 to 50 °C. Energy Build. 52, 107–111. https://doi.org/10.1016/J.ENBUILD.2012.05.029.
Gunderson, P., 1978. Frost Protection of Buried Water and Sewage Pipes (draft translation 666). Cold Region Research and Engineering Laboratory, Hanover, NH, Cold Region Engineering Laboratory report: draft translation 666.
Gwadera, M., Larwa, B., Kupiec, K., 2017. Undisturbed ground temperature—different methods of determination. Sustainability 9, 2055. https://doi.org/10.3390/su9112055.
Hazeni, B., Thomas, J.E., Thornburgs, D.B., 1990. Design and performance of the direct-bury water and sewer utilities in Barrow, Alaska, USA. Nordicana 397–402.
Health Canada, 1995. Guidelines for Canadian Drinking Water Quality: Guideline Technical Document – Temperature.
Johansen, O., 1975. Thermal conductivity of soils. CRREL Draft Transl. 637.
Kennedy, F.E., Phetteplace, G.E., Humiston, N., Prabhakar, V., 1988. Thermal performance of a shallow utilidor, in: International Conference on Permafrost, 5th, Trondheim, Norway, August 2–5, 1988. pp. 1262–1267.
Kuznetsova, E., 2015. Properties of the crushed rocks used as frost protection layer of the Norwegian roads: field and laboratory investigations, in: ECTRI Young Researchers Seminar 2015, 17-19/6/15, Rome, Italy.
Lakatos, A., 2013. Influence of the moisture in the thermal conductivity of Expanded Polystyrene insulators. pp. 653–656.
Leitch, A.F., Heinke, G.W., 1970. Comparison of Utilidors in Inuvik, NWT. Department of Civil Engineering, University of Toronto, Toronto, Ontario.
Lund, H., Werner, S., Wiltshire, R., Svendsen, S., Thorsen, J.E., Hvelplund, F., Mathiesen, B.V., 2014. 4th Generation District Heating (4GDH). Energy 68, 1–11. https://doi.org/10.1016/j.energy.2014.02.089.
Martini, W.R., Churchill, S.W., 1960. Natural convection inside a horizontal cylinder. AIChE J. 6, 251–257.
Mcfadden, T., 1990. The Kilpisjarvi project: case study of cold-regions research in Finland. J. Cold Reg. Eng. 4, 69–84.
Nash, J.E., Sutcliffe, J.V., 1970. River flow forecasting through conceptual models part I — a discussion of principles. J. Hydrol. 10, 282–290. https://doi.org/10.1016/0022-1694(70)90255-6.
Pangborn, R.M., Bertolero, L.L., 1972. Influence of temperature on taste intensity and degree of liking of drinking water. J. Am. Water Works Assoc. 64, 511–515.
Pericault, Y., Hedström, A., Dahl, J., Vesterlund, M., Olsson, G., 2016. District heat tracing of water and sewer lines in Kiruna, Sweden, in: Abstract from Sanitation in Cold Climate Regions, Sisimiut, Greenland. pp. 88–89.
Pericault, Y., Kärrman, E., Viklander, M., Hedström, A., 2018. Expansion of sewer, water and district heating networks in cold climate regions: an integrated sustainability assessment. Sustainability 10, 3743. https://doi.org/10.3390/su10103743.
Pericault, Y., Risberg, M., Vesterlund, M., Viklander, M., Hedström, A., 2017. A novel freeze protection strategy for shallow buried sewer pipes: temperature modelling and field investigation. Water Sci. Technol. 76, 294–301. https://doi.org/10.2166/wst.2017.174.
Reed, S.C., 1977. Field performance of a subarctic utilidor. In: Proceedings, Utilities Delivery in Arctic Regions. Environmental Protection Service Rep. No. EPS 3-WP-77-1, Ottawa, Ontario, pp. 391–438.
Schubert, D., Crum, J., 1996. Freeze protection, thawing and heat tracing. In: Cold Regions Utilities Monograph. p. D-1-D-15. https://doi.org/10.1061/9780784401927.apd.
Schubert, D., Crum, J., Jones, G., Ronimus, A., 2013. Water distribution design and construction in alaska-historic perspectives and current practice. In: ISCORD 2013. American Society of Civil Engineers, pp. 840–851.
SMHI, 2018. Meteorological observations (Meteorologiska observationer, in Swedish). Swedish Meteorogical and Hydrological Institute. [WWW Document]. URL https://opendata-download-metobs.smhi.se/explore/ (accessed 9.25.18).
Smith, D., 1996. Cold Regions Utilities Monograph, Third Edit. ed. American Society of Civil Engineers, New York, NY.
Sundberg, J., 1991. Thermal properties of soil and rock (Termiska egenskaper i jord och berg, in Swedish). Report nr 12 of the Swedish Geotechnical Insitute, Linköping, Sweden.
World Health Organisation, 2008. Guidelines for drinking-water quality, 3rd edition: Volume 1 – Recommendations.